Received: 30 January 2019 | Revised: 30 July 2019 | Accepted: 1 August 2019

DOI: 10.1002/ardp.201900033

DPhG ARCH PHARM
Archiv der Pharmazie

FULL PAPER

Potent ribonucleotide reductase inhibitors: Thiazole-containing thiosemicarbazone derivatives

Merve Ertas[1] | Zafer Sahin[1] | Emre F. Bulbul[1] | Ceysu Bender[1] | Sevde N. Biltekin[2] | Barkin Berk[1] | Leyla Yurttas[3] | Aysu M. Nalbur[4] | Hayati Celik[4] | Şeref Demirayak[1]

[1]Department of Pharmaceutical Chemistry, School of Pharmacy, Istanbul Medipol University, Istanbul, Turkey

[2]Department of Pharmaceutical Microbiology, School of Pharmacy, Istanbul Medipol University, Istanbul, Turkey

[3]Department of Pharmaceutical Chemistry, School of Pharmacy, Anadolu University, Eskişehir, Turkey

[4]Department of Analytical Chemistry, School of Pharmacy, Yeditepe University, Istanbul, Turkey

Correspondence
Merve Ertas, M.Sc., Department of Pharmaceutical Chemistry, School of Pharmacy, Istanbul Medipol University, 34810 İstanbul, Turkey.
Email: mertas@medipol.edu.tr

Funding information
Anadolu University Scientific Research Projects Commission, Grant/Award Number: 1609S624

Abstract

The antioxidant, antimalarial, antibacterial, and antitumor activities of thiosemicarbazones have made this class of compounds important for medicinal chemists. In addition, thiosemicarbazones are among the most potent and well-known ribonucleotide reductase inhibitors. In this study, 24 new thiosemicarbazone derivatives were synthesized, and the structures and purity of the compounds were determined by IR, ^{1}H NMR, ^{13}C NMR, mass spectroscopy, and elemental analysis. The IC_{50} values of these 24 compounds were determined with an assay for ribonucleotide reductase inhibition. Compounds **19**, **20**, and **24** inhibited ribonucleotide reductase enzyme activity at a higher level than metisazone as standard. The cytotoxic effects of these compounds were measured on the MCF7 (human breast adenocarcinoma) and HEK293 (human embryonic kidney) cell lines. Similarly, compounds **19**, **20**, and **24** had a selective effect on the MCF7 and HEK293 cell lines, killing more cancer cells than cisplatin as standard. The compounds (especially **19**, **20**, and **24** as the most active ones) were then subjected to docking experiments to identify the probable interactions between the ligands and the enzyme active site. The complex formation was shown qualitatively. The ADME (absorption, distribution, metabolism, and excretion) properties of the compounds were analyzed using in-silico techniques.

KEYWORDS
antitumor agents, ribonucleotide reductase, thiazole, thiosemicarbazone

1 | INTRODUCTION

As current chemotherapies are not effective against common and aggressive tumors, such as breast, prostate, lung, and brain cancers, research on new compounds focusing on the proliferation of cancerous cells remains crucial. In such research, two main approaches are adopted; either developing new chemotherapeutics targeting DNA or developing the components of cell metabolism and replication.[1] Iron is a key metal that catalyzes important reactions in metabolism, respiration, and oxygen transport as well as DNA synthesis.[2] In cancer cells, the need for iron causes an increase in transferrin receptor 1 that provides intracellular uptake of iron from transferrin.[3–5] In biological systems, iron chelators are responsible for capturing the free iron produced from transferrin and limit the activity of iron-dependent proteins, such as ribonucleotide reductase.

The amount of ribonucleotide reductase determines the rate of cell replication.[6,7] According to Cory and Chiba,[8] ribonucleoside diphosphate reductase inhibitors are better inhibitors of DNA synthesis than DNA polymerase inhibitors.

The antioxidant, antimalarial, antibacterial, and antitumor activities of thiosemicarbazones have made these compounds more interesting for medicinal chemists.[8–32] In addition, with their capability to produce metal complexes, thiosemicarbazones are known to be one of the most potent ribonucleotide reductase enzyme inhibitors.[33]

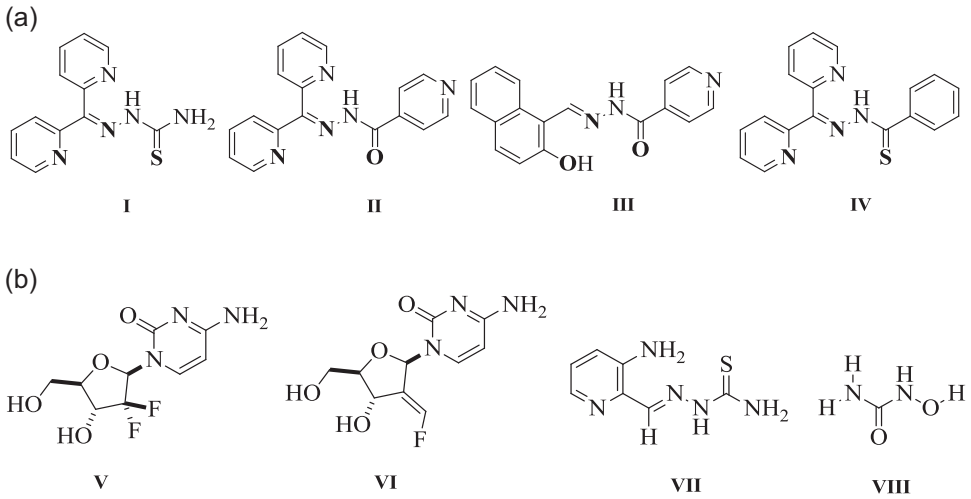

FIGURE 1 (a) Examples of chelators of hydrazones, thiosemicarbazones, and thiohydrazones. Electron-donor atoms are shown in bold. (b) Gemcitabine, MDL 101.731, 3-AP, hydroxyurea structures

Some chelate-producing derivatives of thiosemicarbazones (**I**), hydrazones (**II**, **III**), and thiohydrazones (**IV**) are listed in Figure 1a. These structures create the Fe/ligand complex. Oxidation of metal is primarily dependent on the presence of electron-donating atoms. O, N, O are Fe^{III} chelators of hydrazones, whereas N, N, O are specific to Fe^{II}.[34,35] S (sulfur) acts as an electron-donating precursor specific to iron II and III in thiosemicarbazones and thiohydrazones.

The antitumor activity of thiosemicarbazone derivatives can be explained through two separate mechanisms: In the first, thiosemicarbazides bind to free iron in the cytoplasm and form a redox-active Fe complex by sulfur and two nitrogen atoms, N–N–S.[6,36] The structure–activity relationships of this pattern were examined by Logan et al.[37] in detail, and the –HN–(C═S)–NH– group was shown to be essential for antitumor activity.[37]

In the second mechanism, the target is ribonucleotide reductase enzyme. It binds to iron at high levels and can also be targeted by iron chelators. The ribonucleotide reductase enzyme in mammals consists of two subunits responsible for antitumor activity; part R1 contains polythiols and part R2 contains non-heme iron and the free tyrosyl radical and is the main moiety required for reductase activity. There are also two classes of ribonucleotide reductase inhibitors; nucleoside analogs that bind to the R1 subunit, such as gemcitabine (2′,2′-difluoro-2′-deoxycytidine; **V**) and MDL 101.731 (2′-fluoromethylene-2′-deoxydidine; **VI**), and those that bind to either the non-heme iron or the free radicals in the R2 subunit; for example, heterocyclic carboxaldehyde thiosemicarbazone 3-AP (**VII**), 3-aminopyridine-2-carboxyaldehyde thiosemicarbazone, and *N*-hydroxyurea (**VIII**). Heterocyclic carboxaldehyde thiosemicarbazones have been found to be more effective inhibitors compared to *N*-hydroxyurea, which has a relatively short half-life (Figure 1b).[38–43]

In this study, 24 novel thiosemicarbazone analogs were synthesized, and their cytotoxic activities were assessed on the human embryonic kidney (HEK293) and human breast cancer (MCF7) cell lines. Ribonucleotide reductase enzyme inhibition activities were evaluated at 10 μM concentration compared to metisazone. As the active compounds gave similar results in both tests, a docking study was also performed to clarify the possible interactions between the active site and the molecules.

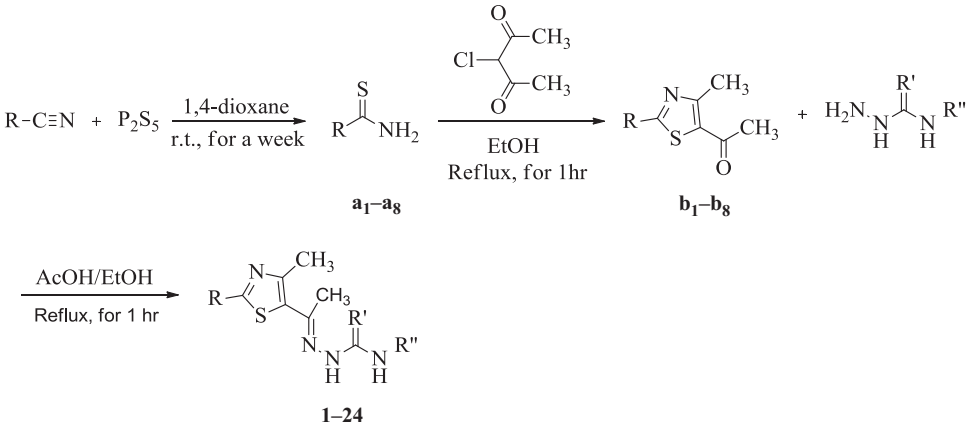

SCHEME 1 Synthesis pathway of compounds **1–24**

TABLE 1 Structures of compounds **1–24**

Compound	R	R′	R″
1	4-Cl phenyl	S	H
2	4-OCH_3 phenyl	S	H
3	2-Pyridyl	S	H
4	3-Pyridyl	S	H
5	4-Pyridyl	S	H
6	2-Pyrazinyl	S	H
7	2-Pyrimidinyl	S	H
8	Phenyl	S	H
9	4-Cl phenyl	O	Phenyl
10	4-OCH_3 phenyl	O	Phenyl
11	2-Pyridyl	O	Phenyl
12	3-Pyridyl	O	Phenyl
13	4-Pyridyl	O	Phenyl
14	2-Pyrazinyl	O	Phenyl
15	2-Pyrimidinyl	O	Phenyl
16	Phenyl	O	Phenyl
17	4-Cl phenyl	S	CH_3
18	4-OCH_3 phenyl	S	CH_3
19	2-Pyridyl	S	CH_3
20	3-Pyridyl	S	CH_3
21	4-Pyridyl	S	CH_3
22	2-Pyrazinyl	S	CH_3
23	2-Pyrimidinyl	S	CH_3
24	Phenyl	S	CH_3

Furthermore, stoichiometric analysis of complexes belonging to metisazone, compounds **1**, **19**, **20**, and **24,** and Fe(III) was undertaken. Finally, the ADME properties of the compounds were analyzed using in-silico techniques.

2 | RESULTS AND DISCUSSION

2.1 | Chemistry

The synthetic pathway and structures of the final thiazolylmethyl-ketone-(thio)semicarbazones (compounds **1–24**) are detailed in Scheme 1 and Table 1, respectively. Initially, aryl-substituted carbonitriles were reacted with phosphorus pentasulfide in 1,4-dioxane to produce aryl-substituted thioamide derivatives ($\mathbf{a_1}$–$\mathbf{a_8}$). Then, 1-(2-aryl-4-methylthiazol-5-yl)ethanone derivatives ($\mathbf{b_1}$–$\mathbf{b_8}$) were obtained by the synthesis of aryl thioamides and 3-chloro-2,4-pentanedione. Finally, 1-(2-aryl-4-methylthiazol-5-yl)ethanones and (thio)semi-carbazide derivatives were reacted together using an acetic acid catalyst to acquire compounds **1–24**.[20,44] The structures and purity of these novel compounds were elucidated by the spectroscopic methods of infrared (IR), ^{1}H NMR, ^{13}C NMR, and mass and elemental analysis.

2.2 | Anticancer activity assay

To assess the cytotoxic activity of compounds on the HEK293 and MCF7 cell lines, various concentrations (5×10^{-4}–10^{-6} M) were applied to the medium. The IC_{50} cytotoxicity values were considered to be the compound concentrations that reduced the absorbance to 50% compared with the level in untreated control wells and were derived from at least six separate experiments. The control group cells that contained nothing incubated at 37°C were accepted as having 100% viability. The effect of the compounds' IC_{50} values is presented in Table 2. Statistical comparisons were made using one-way analysis of variance and a module of the GraphPad Prism software version 7.02 (La Jolla, CA). Differences in the mean values were considered to be significant when $p < 0.05$.

When the 48-hr effect of the substances was assessed on the MCF7 and HEK293 cell lines, the toxicity of most of the compounds

TABLE 2 IC_{50} values (μM) of the substances in the HEK293 and MCF7 cell lines

Compound	MCF7	HEK293	Compound	MCF7	HEK293
1	14.2 ± 1.4	55.9 ± 2.2	**13**	62.1 ± 1.5	57.9 ± 1.9
2	10.4 ± 0.33	21 ± 5.1	**14**	34.2 ± 3.5	28.4 ± 2.1
3	19.2 ± 2.4	53.1 ± 3.3	**15**	56.5 ± 2.2	51.9 ± 2.4
4	7 ± 1.33	8.6 ± 3.4	**16**	12.4 ± 1.3	15.3 ± 3.9
5	16.1 ± 2	57.9 ± 4.2	**17**	19.2 ± 3.5	50.1 ± 3.2
6	12.5 ± 0.9	11 ± 0.4	**18**	7.9 ± 1.1	18.2 ± 3.4
7	37.4 ± 1.2	45 ± 4.1	**19**	**1.4 ± 0.25**	23.4 ± 1.1
8	17 ± 4.2	10.2 ± 2	**20**	**4.1 ± 0.9**	33.4 ± 5.1
9	58.3 ± 2.2	50.9 ± 3.2	**21**	**4.5 ± 2**	38.4 ± 4.4
10	19.5 ± 2	15.4 ± 2.3	**22**	7.4 ± 1.3	45.4 ± 3
11	63.7 ± 0.2	56.1 ± 2.5	**23**	11.2 ± 2	50.2 ± 2.2
12	55.1 ± 3.2	41.4 ± 5.2	**24**	**2.4 ± 0.1**	13 ± 0.9
Cisplatin*	5.75 ± 0.02	10.51 ± 1.31			

Note: Asterisk represents the standart. Bold figures mean significant values.

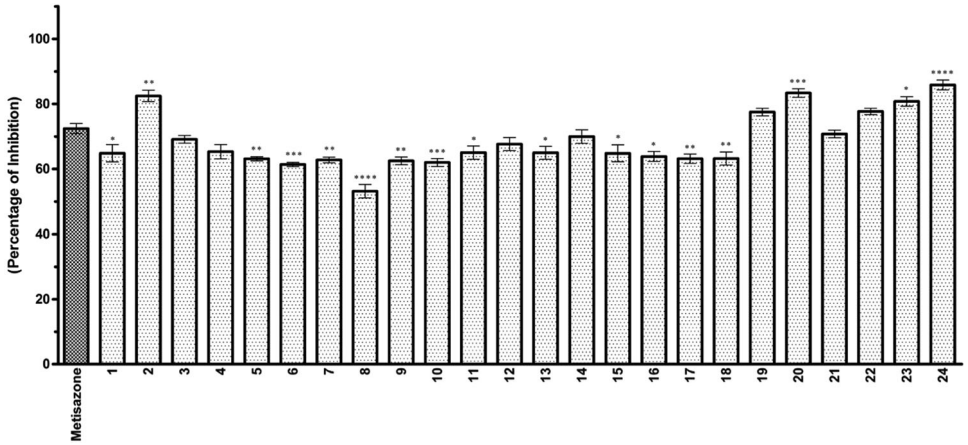

FIGURE 2 The results of the enzyme inhibition assays of 10 μM of the standard inhibitor metisazone and 24 substances. Vertical bars showing standard deviation values. *$p < 0.05$, **$p < 0.01$, ***$p < 0.001$, ****$p < 0.0001$

was more selective for cancer cells than for normal cells. The IC_{50} values of compounds **19**, **20**, **21**, and **24** in the MCF7 cells were lower compared to the standard substance, cisplatin. While the IC_{50} values of compounds **20** and **21** were very close to that of cisplatin, the IC_{50} value of compound **24** was 2.4 μM, which was almost half the value of the standard. The IC_{50} value of the most active compound (**19**) was 1.4 μM. This compound also had a higher IC_{50} value in the HEK293 cell line.

2.3 | Ribonucleotide reductase enzyme inhibition activity

The ribonucleotide reductase enzyme inhibition activity of 24 compounds and the standard metisazone (% inhibition = 77.44) was measured at a concentration of 10 μM. For this purpose, the standard from the kit was diluted at various dilutions. A standardized graph was plotted based on the results (R^2: 0.9809). The values obtained as a result of the experimental studies were evaluated according to this graph. The values obtained are given in Figure 2 and Table 3.

Compound **24** was the most potent inhibitor of ribonucleotide reductase activity (85.85% inhibition). Other compounds with higher activity than metisazone were compounds **20** (83.34% inhibition), **2** (82.46%), **23** (80.77%), **22** (77.69%), and **19** (77.50%). Compound **8** had the least-inhibiting effect on ribonucleotide reductase activity (~50% inhibition).

2.4 | Molecular docking studies

Docking experiments were undertaken with all synthesized compounds and 1W68 to identify the possible interaction patterns on the largest active site closer to Fe found with the Site Map. The experiments were initially performed using the SP algorithm of Glide, treating the receptor as rigid and the ligands as flexible. The enclosing box was centered on the center of the largest binding site, and default sizes were used for both the enclosing and bounding boxes. All ligands seemed to fit well into the pocket, giving similar poses (Figure 3).

The binding site between two helical secondary structures seem to produce two hydrophobic cavities connected with a narrow hydrophobic tunnel. Therefore a three compartment structure, seemingly, can best fit horizontally to this binding site. The vertical positioning of functional groups belong to Phe 241, Tyr 324, and Asn 346 with Phe 245 seem to lock the positioning of the central thiazole moiety with hydrophobic interactions. The nitrogen atom of the

TABLE 3 Ten-micromolar enzyme inhibition values of metisazone, used as a standard inhibitor, and the derived substances

Compound	% Inhibition	Compound	% Inhibition	Compound	% Inhibition
1	64.83 ± 4.58	**9**	62.49 ± 2.08	**17**	63.16 ± 2.52
2	**82.46 ± 3.06**	**10**	61.98 ± 2.16	**18**	63.22 ± 3.46
3	69.12 ± 2.08	**11**	65.04 ± 3.51	**19**	**77.50 ± 2.00**
4	65.33 ± 3.79	**12**	67.65 ± 3.46	**20**	**83.34 ± 2.31**
5	63.12 ± 1.15	**13**	64.97 ± 3.46	**21**	70.78 ± 2.08
6	61.38 ± 1.15	**14**	69.96 ± 3.61	**22**	**77.69 ± 1.73**
7	62.75 ± 1.53	**15**	64.80 ± 4.51	**23**	**80.77 ± 2.50**
8	53.16 ± 3.61	**16**	63.84 ± 2.65	**24**	**85.85 ± 2.65**
Metisazone*	72.44				

Note: Asterisk represents the standart. Bold figures mean significant values.

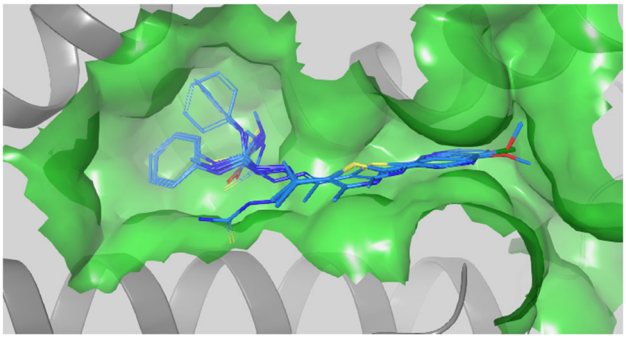

FIGURE 3 Poses of all compounds in the active site

thiosemicarbazone moiety binds with a hydrogen bond to the *p*-OH group of the Tyr 324 in all compounds. Aromatic functional groups, pyrimidine, pyridine, and phenyl, which are directly connected to the thiazole ring system, position themselves in the shallow cavity surrounded by Phe 348, Lys 249, Trp 246, and Phe 245 with hydrophobic interactions. However, the substitution on these ring systems can produce van der Waals clashes with the side chains and are not favored. On the contrary, the cavity produced by Phe 327, Val 328, Arg 331, Phe 237, and Ser 238 is deeper. This pocket can easily host freely rotating over a single-bond ring system such as phenyl, though the smaller hydrophobic functional groups are capable of creating the same hydrophobic interactions. The lowest IC_{50} values during ribonucleotide reductase inhibition were obtained from compounds **19**, **20**, and **24,** therefore two- and three-dimensional (3D) interaction patterns for these compounds are given in Figures 4 and 5 representing all the compounds.

2.5 | Absorption spectra and stoichiometry of complexes

The complex formation between Fe(III) ions and the ligands/metisazone was investigated. For representative purposes, the experimental details of compound **1** are given in Figure 6a as the same results were obtained from other ligands including metisazone. This figure shows the absorption spectra of the Fe(III)–compound **1** complex recorded in the wavelength range of 200 to 400 nm.

The stoichiometry of the Fe(III)–compound **1** complex was determined by continuous variation of the compound **1** concentration while keeping the concentration of the Fe(III) ions constant. The complex had a maximum absorbance at 343 nm. The stoichiometric ratio between the metal and ligand was found by plotting the absorbance values at 343 nm versus mole ratio (Figure 6b).

The plot obtained by the molar ratio method indicated that the ligand and metal ions formed the complex at a molar ratio of 1:4. In this study, we only showed the complex formation between ferric ions and ligands. The determination of conditional stability constants

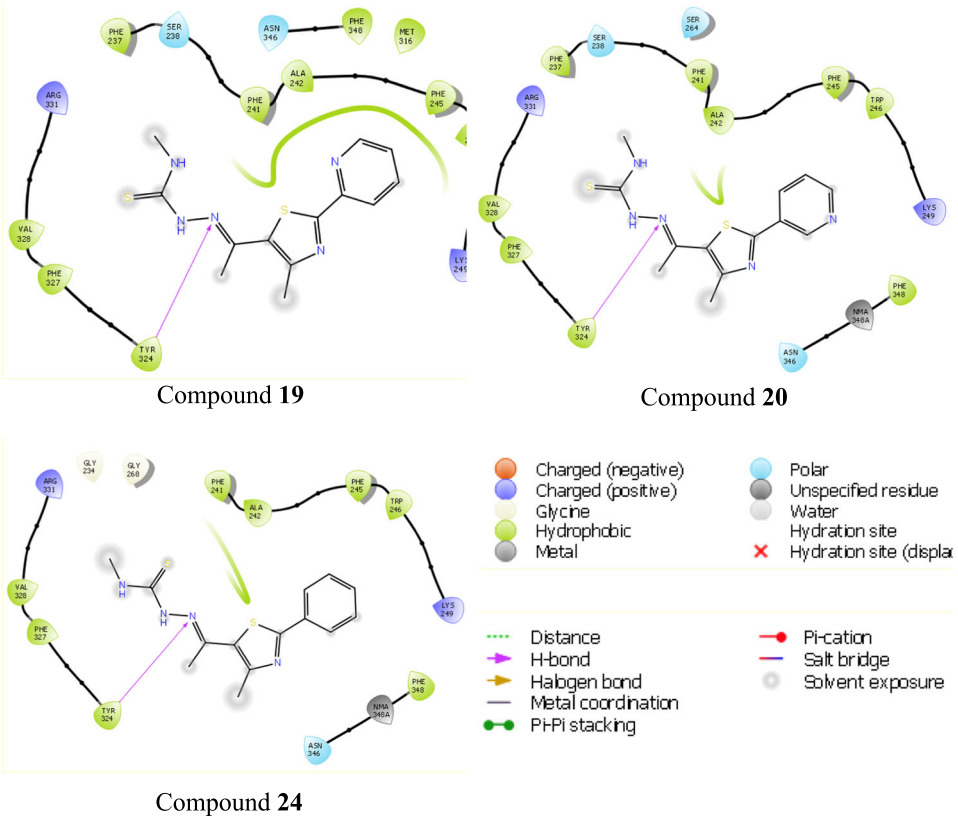

FIGURE 4 Two-dimensional interaction diagrams for compounds **19**, **20**, and **24**

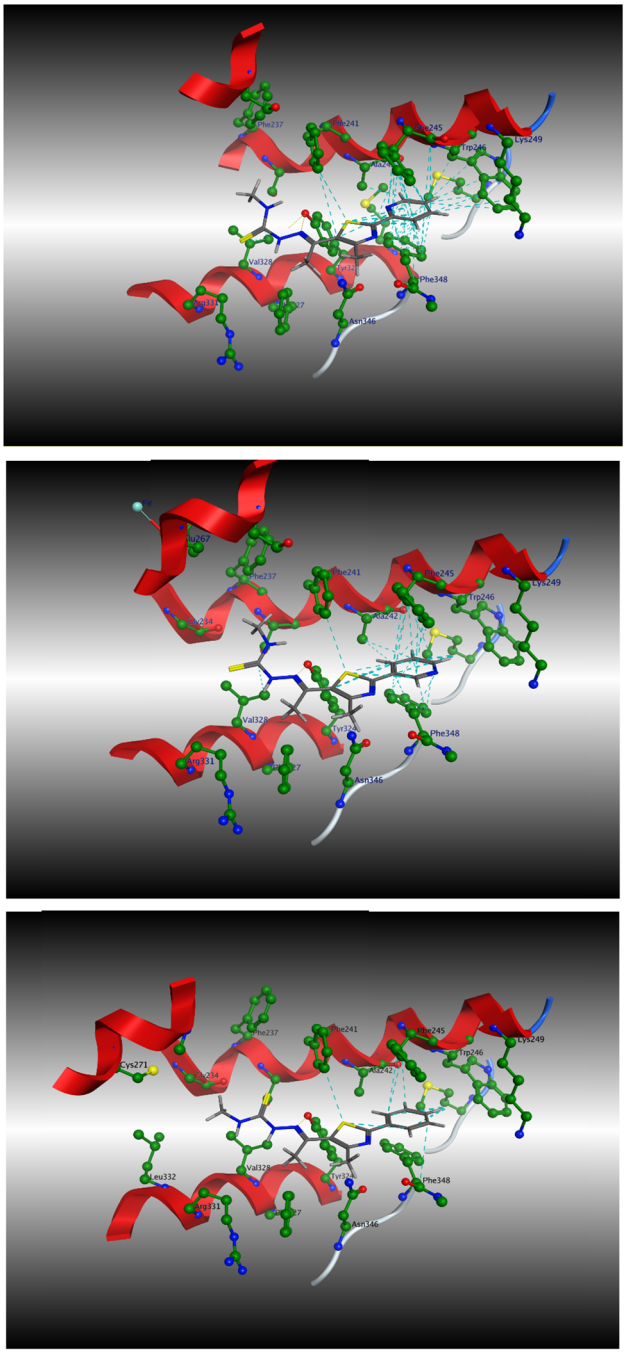

FIGURE 5 Three-dimensional interaction diagrams for compounds **19**, **20**, and **24**

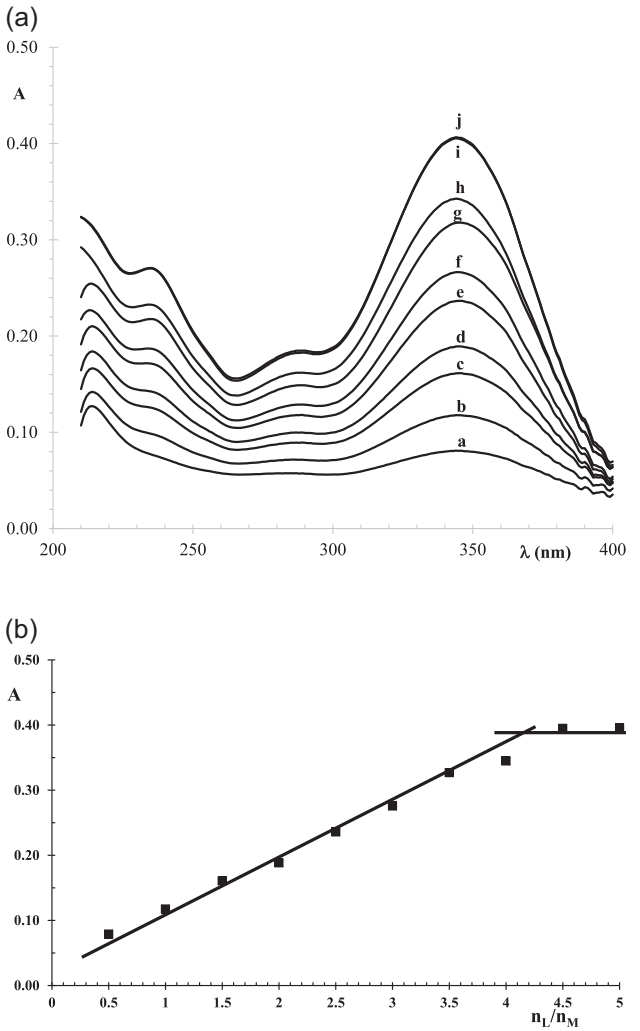

FIGURE 6 (a) Absorption spectra of Fe(III)–compound **1** complex in the presence of 10% ethanol in a buffer solution at pH 7.40. Mole ratios (n_L/n_M): (a) 0.5, (b) 1.0, (c) 1.5, (d) 2.0, (e) 2.5, (f) 3.0, (g) 3.5, (h) 4.0, (i) 4.5, and (j) 5.0. (b) Molar ratio method: $[Fe^{3+}]$ = 0.002 mM and [L] = 0.001–0.010 mM in phosphate buffer at pH 7.40. A on the *y*-axis means absorption

and formation of complexes with other metals ions, including nickel, copper, cobalt, and lead is currently under investigation.

2.6 | Theoretical calculation of the absorption, distribution, metabolism, and excretion (ADME) parameters

Poor pharmacokinetics is one of the major causes of failure in the costly late-stage drug development process. Therefore, the pharmacokinetic profiles of potential novel drugs should be evaluated as early as possible in the drug development process. Studies conducted in recent years have shown a significant increase in the number of compounds required for early delivery of ADME.[45] For this reason, we analyzed the ADME properties of compounds **1–24** using the online Molinspiration property calculator, which allows easy interactive determination of molecular properties.[46] Lipinski's rule of five was also employed using this software. This set of rules require that an orally active drug should not violate more than one criterion.[47] The ADME parameters of molecular weight, topological polar surface area (tPSA), number of hydrogen donors, number of hydrogen acceptors, number of rotatable bonds, and volume were calculated theoretically and evaluated in accordance with Lipinski's rule (Table 4). According to the results, none of the compounds (**1–24**) violated more than one criterion. Thus, this analysis confirmed the biological significance of compounds **19**, **20**, and **24** having a good pharmacological profile.

TABLE 4 Physicochemical properties of compounds **1–24** used in the prediction of ADME profiles

Compound	MW	tPSA	nON	nOHNH	Vol	nrotb	Vio
1	324.86	63.31	4	3	263.48	4	0
2	320.44	72.54	5	3	275.49	5	0
3	291.40	76.20	5	3	245.79	4	0
4	291.40	76.20	5	3	245.79	4	0
5	291.40	76.20	5	3	245.79	4	0
6	292.39	89.09	6	3	241.63	4	0
7	292.39	89.09	6	3	241.63	4	0
8	290.42	63.31	4	3	249.94	4	0
9	384.89	66.38	5	2	327.12	4	1
10	380.47	75.61	6	2	339.13	5	0
11	351.44	79.27	6	2	309.43	4	0
12	351.44	79.27	6	2	309.43	4	0
13	351.44	79.27	6	2	309.43	4	0
14	352.42	92.17	7	2	305.27	4	0
15	352.42	92.17	7	2	305.27	4	0
16	350.45	66.38	5	2	313.59	4	0
17	338.89	49.31	4	2	281.15	5	0
18	334.47	58.54	5	2	293.16	6	0
19	305.43	62.20	5	2	263.46	5	0
20	305.43	62.20	5	2	263.46	5	0
21	305.43	62.20	5	2	263.46	5	0
22	306.42	75.09	6	2	259.30	5	0
23	306.42	75.09	6	2	259.30	5	0
24	304.44	49.31	4	2	267.62	5	0

Abbreviations: ADME, absorption, distribution, metabolism, and excretion; MW, molecular weight; nOHNH, number of hydrogen donors; nON, number of hydrogen acceptors; nrotb, number of rotatable bonds; tPSA, total polar surface area; Vio, Violation; Vol, molecular volume.

For evaluating the drug-likeness properties of the compounds, the QikProp module of Maestro was used, and the results are presented in Table 5.

The results obtained from this study indicate that the compounds may have an effect on CNS as well as showing K^+ channel inhibitor activity and binding to human serum albumin. The brain/blood partition coefficient and high oral absorption values were within the acceptable range of drug-likeness.

3 | CONCLUSION

In this study, novel thiazolylmethylketone(thio)semicarbazone derivatives were synthesized by reacting acetylthiazole derivatives with thiosemicarbazides. The structure and purity of the obtained compounds was determined by IR, ^{1}H NMR, ^{13}C NMR, mass spectroscopy, and elemental analysis. The effect of the compounds on cellular proliferation was monitored using the Cell Proliferation Reagent Kit I. Compounds **19**, **20,** and **24** had a selective effect on the MCF7 and HEK293 cell lines, killing cancer cells more than the cisplatin standard. The ribonucleotide reductase inhibition effect of the compounds targeted with the RRM2 ELISA kit was examined using metisazone as standard. Compounds **19**, **20**, and **24** inhibited ribonucleotide reductase enzyme activity at a higher level than the standard. Molecular docking studies on the selected most active compounds (**19**, **20**, and **24**) revealed good docking poses. The complex formation between the metal ion and these compounds (including metisazone) was shown quantitatively. Furthermore, the ADME parameters were calculated and these molecules were found to have a good pharmacokinetic profile. The results indicated that (thio)semicarbazone containing sulfur and small hydrophobic moieties inhibit ribonucleotide reductase activity effectively, as observed in compounds **19**, **20**, and **24** in this study.

4 | EXPERIMENTAL

4.1 | Chemistry

4.1.1 | General

All chemicals used were purchased from Aldrich Chemical Co. (Steinheim, Germany). Melting points were determined with a Stuart melting point apparatus SMP30 (Staffordshire, UK). IR spectra (KBr) were recorded on a PerkinElmer spectrum two FT-IR spectrometer (Waltham, MA), and ^{1}H-NMR spectra were obtained with a Bruker DPX-500, 300 MHz High-Performance Digital FT-NMR. ^{13}C-NMR spectra were measured using a DPX-125, 75 MHz high-performance digital FT-NMR. All the chemical shift values were recorded as δ (ppm). Mass spectra were obtained using an Agilent 1100 MSD series mass spectrometer. The purity of the compounds was checked by thin-layer chromatography on silica gel-coated aluminum sheets (Merck, 1.005554, silica gel HF254–361, Type 60, 0.25 mm; Darmstadt, Germany). Elemental analyses were performed with a Leco CHNS 932 analyzer (Leco Corp., MI) and were found to be within ± 0.4% of the theoretical values for C, H, and N.

The original IR and NMR spectra are provided as Supporting Information, as are the InChI codes of the investigated compounds together with some biological activity data.

4.1.2 | General procedure for the synthesis of thioamide derivatives (a_{1-8})

Carbonitrile derivatives (10 mmol) were stirred in 1,4-dioxane (40 ml) with P_2S_5 (10 mmol) for 1 week at room temperature. Ice was added to the resulting product. The solution was neutralized with ammonia and the crude product was obtained by filtration.

4.1.3 | General procedure for the synthesis of thiazole derivatives (b_{1-8})

The thioamide derivatives (5 mmol) were refluxed with 3-chloro-2,4-pentanedione (5 mmol) in ethanol. The obtained product was cooled, filtered, and washed with ethanol.

TABLE 5 Predicted drug-likeness properties of the compounds **1–24**

Compound	CNS	logPo/w	$\log_{HERG}$	P_{Caco}	logBB	PMDCK	$\log_{KHSA}$	HOA	%HOA
1	0	3.651	−5.785	1,762.828	0.033	10,000	0.16	3	100
2	−1	2.949	−5.214	1,764.07	−0.197	3,503.967	0.002	3	100
3	−1	2.245	−5.283	998.017	−0.367	2,042.255	−0.182	3	93.767
4	−1	1.928	−5.145	754.08	−0.49	1,432.696	−0.254	3	89.736
5	−1	1.925	−5.142	754.042	−0.49	1,431.647	−0.255	3	89.719
6	−1	1.399	−5.057	523.723	−0.646	1,014.433	−0.406	3	83.801
7	−1	1.647	−5.153	614.148	−0.584	1,210.466	−0.339	3	86.491
8	−1	2.823	−5.276	1,765.753	−0.114	3,500.883	−0.029	3	100
9	0	4.88	−5.51	1,348.86	−0.233	3,613.102	0.64	1	100
10	0	4.448	−5.435	1,347.696	−0.466	1,465.214	0.529	3	100
11	0	3.826	−5.511	983.171	−0.54	1,079.678	0.324	3	100
12	0	3.485	−5.411	726.401	−0.69	751.664	0.228	3	100
13	0	3.485	−5.41	724.81	−0.691	750.423	0.228	3	100
14	−1	2.921	−5.308	519.647	−0.846	541.789	0.032	3	92.655
15	−1	3.192	−5.389	609.176	−0.775	643.512	0.124	3	95.479
16	0	4.384	−5.609	1,347.695	−0.393	1,465.214	0.522	3	100
17	1	3.985	−5.336	3,205.332	0.281	10,000	0.279	3	100
18	1	3.583	−5.266	3,203.695	0.046	6,005.222	0.189	3	100
19	0	2.99	−5.317	2,302.331	−0.028	4,299.548	−0.017	3	100
20	0	2.626	−5.193	1,746.449	−0.177	2,679.481	−0.081	3	100
21	0	2.625	−5.187	1,750.214	−0.175	2,697.81	−0.083	3	100
22	0	2.043	−5.115	1,197.232	−0.316	2,135.208	−0.287	3	94.003
23	0	2.325	−5.171	1,449.935	−0.257	2,290.109	−0.184	3	100
24	1	3.515	−5.399	3,257.18	0.098	5,275.57	0.193	3	100

Note: Predicted central nervous system (CNS) activity on a scale of −2 (inactive) to +2 (active); PlogPo/w, predicted octanol/water partition coefficient (−2.0 to 6.5); $\log_{HERG}$, predicted IC_{50} value for blockage of HERG K^+ channels (below −5); logBB, predicted brain/blood partition coefficient (−3.0 to 1.2); $\log K_{HSA}$, prediction of binding to human serum albumin (−1.5 to 1.5); Human Oral Absorption (HOA), predicted qualitative human oral absorption measured as 1, 2, or 3 for low; Percent HOA, high if >80% and poor if <25%.

4.1.4 | General procedure for the synthesis of the thiazolylmethylketone(thio)semicarbazones 1–24

4-Acetyl-5-methylthiazole derivatives (3 mmol) were refluxed with (thio)semicarbazide derivatives in ethanol by an acetic acid catalyst. The resulting product was filtered and washed with ethanol.[20,44]

*2-(1-(2-(4-Chlorophenyl)-4-methylthiazole-5-yl)ethylidene)hydrazinecarbothioamide (**1**)*

Yield, 70–74%; m.p. 220.9°C. IR V_{max} (cm^{-1}): 3,411 (NH), 3,283–3,151.7 (arom.), 2,968–2,912.1 (aliph.), 1,582.30–1,493.57 (C═N, C═C), 1,087.95 (C═S), 692.81 (C–S), and 531.23 (C–Cl). ^{1}H-NMR (300 MHz, DMSO-d_6) δ (ppm): 2.39 (3H, s, CH_3), 2.60 (3H, s, thiazole CH_3), 7.44 (1H, brs, NH), 7.54–7.58 (2H, m, phenyl $C_{3,5}$–H), 7.91–7.95 (2H, m, phenyl $C_{2,6}$–H), and 8.41 (1H, brs, NH). ^{13}C-NMR (75 MHz, DMSO-d_6) δ (ppm): 17.87, 18.67, 128.12, 129.79, 131.99, 132.79, 135.46, 143.77, 152.34, 163.42, and 179.31. Mass (ESI), *m/z*: 325.0345 (M^+). Anal. calcd. for C, 48.06; H, 4.03; Cl, 10.91; N, 17.25; S, 19.74. Found: C, 48.08; H, 4.01; Cl, 10.93; N, 17.24; S, 19.75.

*2-(1-(2-(4-Methoxyphenyl)-4-methylthiazole-5-yl)ethylidene)hydrazinecarbothioamide (**2**)*

Yield, 66–68%; m.p. 224.8°C. IR V_{max} (cm^{-1}): 3,266,5 (NH), 3,132 (arom.), 2,958–2,833.4 (aliph.), 1,605.23–1,499.96 (C═N, C═C), 1,171.87 (C–O), 1,087.41 (C═S), and 706.53 (C–S). ^{1}H-NMR (300 MHz, DMSO-d_6) δ (ppm): 2.37 (3H, s, CH_3), 2.58 (3H, s, thiazole CH_3), 3.82 (3H, s, OCH_3), 7.03–7.06 (2H, m, phenyl $C_{3,5}$–H), 7.40 (1H, s, NH), 7.84–7.88 (2H, m, phenyl $C_{2,6}$–H), and 8.38 (1H, brs, NH). ^{13}C NMR (75 MHz, DMSO-d_6) δ (ppm): 17.90, 18.73, 55.90, 115.07, 75.98, 128.11, 131.11, 144.16, 152.07, 161.56, 164.87, and 179.21. Mass (ESI), *m/z*: 321.0836 (M^+). Anal. calcd. for C, 52,48; H, 5.03; N, 17.48; O, 4.99; S, 20.01. Found: C, 52.49; H, 5.02; N, 17.49; O, 5.00; S, 20.00.

*2-(1-(4-Methyl-2-(pyridine-2-yl)thiazole-5-yl)ethylidene)hydrazine carbothioamide (**3**)*

Yield, 72–74%; m.p. 218.2°C. IR V_{max} (cm^{-1}): 3,233.7 (NH), 3,115.6–3,053.2 (arom.), 2,912.1–2,767.7 (aliph.), 1,688–1,619.1 (C═N, C═C), 1,088.35 (C═S), and 781.18 (C–S). ^{1}H NMR (300 MHz,

DMSO-d_6) δ (ppm): 2.40 (3H, s, CH_3), 2.62 (3H, s, thiazole CH_3), 7.47–7.52 (2H, m, pyridine C_4–H, NH), 7.95 (1H, td, J = 7.50, 1.68 Hz, pyridine C_5–H), 8.10 (1H, d, J = 7.82 Hz, pyridine C_3–H), 8.39 (1H, s, NH), and 8.61 (1H, d, J = 4.85 Hz, pyridine C_6–H). ^{13}C NMR (75 MHz, DMSO-d_6) δ (ppm): 18.15, 18.90, 119.46, 75.71, 134.24, 138.20, 143.90, 150.22, 150.70, 152.58, 165.89, and 179.35. Mass (ESI), *m/z*: 292.0679 (M^+). Anal. calcd. for C, 49.46; H, 4.50; N, 24.03; S, 22.01. Found: C, 49.49; H, 4.51; N, 24.05; S, 22.00.

*2-(1-(4-Methyl-2-(pyridine-3-yl)thiazole-5-yl)ethylidene)hydrazinecarbothioamide (**4**)*

Yield, 74–78%; m.p. 202°C. IR V_{max} (cm^{-1}): 3,240.3 (NH), 3,151.7 (arom.), 2,981 (aliph.), 1,489.62–1,476.66 (C═N, C═C), 1,084.2 (C═S), and 703.90 (C–S). ^{1}H NMR (300 MHz, DMSO-d_6) δ (ppm): 2.40 (3H, s, CH_3), 2.62 (3H, s, thiazole CH_3), 7.45–7.55 (2H, m, pyridine C_4–H, NH), 8.27 (1H, d, J = 7.73 Hz, pyridine C_5–H), 8.44 (1H, brs, NH), 8.66 (1H, d, J = 5.05 Hz, pyridine C_6–H), and 9.10 (1H, s, pyridine C_2–H). ^{13}C NMR (75 MHz, DMSO-d_6) δ (ppm): 17.87, 18.63, 124.72, 129.13, 133.21, 133.81, 143.66, 147.19, 151.48, 152.43, 161.78, and 179.35. Mass (ESI), *m/z*: 292.0688 (M^+). Anal. calcd. for C, 49.46; H, 4.50; N, 24.03; S, 22.01. Found: C, 49.49; H, 4.51; N, 24.05; S, 22.00.

*2-(1-(4-Methyl-2-(pyridine-4-yl)thiazole-5-yl)ethylidene)hydrazinecarbothioamide (**5**)*

Yield, 68–72%; m.p. 221.1°C. IR V_{max} (cm^{-1}): 3,417.5 (NH), 3,250.1–3,138.6 (arom.), 2,977.8 (aliph.), 1,691.3–1,595.84 (C═N, C═C), 1,078.84 (C═S), and 715.72 (C–S). ^{1}H NMR (300 MHz, DMSO-d_6) δ (ppm): 2.40 (3H, s, CH_3), 2.63 (3H, s, thiazole CH_3), 7.47 (1H, brs, NH), 7.84 (2H, d, J = 5.57 Hz, pyridine $C_{3,5}$–H), 8.44 (1H, brs, NH), and 8.70 (2H, d, J = 6.12 Hz, pyridine $C_{2,6}$–H). ^{13}C NMR (75 MHz, DMSO-d_6) δ (ppm): 17.90, 18.67, 120.21, 134.42, 139.62, 143.42, 151.23, 152.78, 161.95, and 179.41. Mass (ESI), *m/z*: 292.0683 (M^+). Anal. calcd. for C, 49.46; H, 4.50; N, 24.03; S, 22.01. Found: C, 49.49; H, 4.51; N, 24.05; S, 22.00.

*2-(1-(4-Methyl-2-(pyrazine-2-yl)thiazole-5-yl)ethylidene)hydrazinecarbothioamide (**6**)*

Yield, 68–72%; m.p. 232.6°C. IR V_{max} (cm^{-1}): 3,414.2 (NH), 3,194.3–3,135.3 (arom.), 3,046.7–2,987.6 (aliph.), 1,588.02–1,501.61 (C═N, C═C), 1,084.72 (C═S), and 719.96 (C–S). ^{1}H NMR (300 MHz, DMSO-d_6) δ (ppm): 2.40 (3H, s, CH_3), 2.64 (3H, s, thiazole CH_3), 7.51 (1H, s, NH), 8.41 (1H, s, NH), 8.69 (1H, d, J = 2.78 Hz, pyrazine C_5–H), 8.73 (1H, d, J = 2.64 Hz, pyrazine C_6–H), and 9.27 (1H, s, pyrazine C_3–H). ^{13}C NMR (75 MHz, DMSO-d_6) δ (ppm): 18.10, 18.83, 135.32, 140.79, 143.53, 145.03, 146.10, 146.31, 153.01, 163.16, and 179.41. Mass (ESI), *m/z*: 293.0633 (M^+). Anal. calcd. for C, 45.19; H, 4.14; N, 28.74; S, 21.93. Found: C, 45.16; H, 4.15; N, 28.77; S, 21.96.

*2-(1-(4-Methyl-2-(pyrimidine-4-yl)thiazole-5-yl)ethylidene)hydrazinecarbothioamide (**7**)*

Yield, 72–76%; m.p. 252.5°C. IR V_{max} (cm^{-1}): 3,427.3 (NH), 3,112.3–3,033.5 (arom.), 2,971.2 (aliph.), 1,668.4–1,600.48 (C═N, C═C), 1,078.84 (C═S), and 806.38 (C–S). ^{1}H NMR (300 MHz, DMSO-d_6) δ (ppm): 2.41 (3H, s, CH_3), 2.64 (3H, s, thiazole CH_3), 7.52 (1H, s, NH), 7.57 (1H, t, J = 4.76 Hz, pyrimidine C_5–H), 8.41 (1H, brs, NH), and 8.92 (2H, d, J = 4.76 Hz, pyrimidine $C_{4,6}$–H). ^{13}C NMR (75 MHz, DMSO-d_6) δ (ppm): 18.18, 18.92, 122.04, 135.86, 143.57, 153.25, 158.57, 158.91, 163.33, and 179.42. Mass (ESI), *m/z*: 293.0648 (M^+). Anal. calcd. for C, 45.19; H, 4.14; N, 28.74; S, 21.93. Found: C, 45.16; H, 4.16; N, 28.70; S, 21.95.

*2-(1-(4-Methyl-2-phenylthiazole-5-yl)ethylidene)hydrazinecarbothioamide (**8**)*

Yield, 68–70%; m.p. 221.7°C. IR V_{max} (cm^{-1}): 3,447 (NH), 3,322.3–3,197.6 (arom.), 2,977.8–2,902.3 (aliph.), 1,573.2–1,487.58 (C═N, C═C), 1,080.16 (C═S), and 753.51 (C–S). ^{1}H-NMR (300 MHz, DMSO-d_6) δ (ppm): 2.39 (3H, s, CH_3), 2.61 (3H, s, thiazole CH_3), 7.44 (1H, s, NH), 7.47–7.52 (3H, m, phenyl $C_{3,4,5}$–H), 7.91–7.94 (2H, m, phenyl $C_{2,6}$–H), and 8.41 (1H, s, NH). ^{13}C NMR (75 MHz, DMSO-d_6) δ (ppm): 17.93, 18.73, 126.45, 129.72, 130.95, 132.25, 133.17, 143.94, 152.25, 164.83, and 179.29. Mass (ESI), *m/z*: 291.0729 (M^+). Anal. calcd. for C, 53.77; H, 4.86; N, 19.29; S, 22.08. Found: C, 53.75; H, 4.88; N, 19.30; S, 22.10.

*2-(1-(2-(4-Chlorophenyl)-4-methylthiazole-5-yl)ethylidine)-N-phenylhydrazinecarboxamide (**9**)*

Yield, 76–78%; m.p. 191.6°C. IR V_{max} (cm^{-1}): 3,368.3 (NH), 3,263.3–3,175.92 (arom.), 2,977.8 (aliph.), 1,644.07 (C═O), 1,620.23–1,506.62 (C═N, C═C), 716.68 (C–S), and 565.95 (C–Cl). ^{1}H-NMR (300 MHz, DMSO-d_6) δ (ppm): 2.39 (3H, s, CH_3), 2.60 (3H, s, CH_3), 7.18 (2H, s, H_{Ar}), 7.55–7.58 (3H, d, J = 9 Hz, H_{Ar}), 7.92–7.95 (2H, d, J = 9 Hz, H_{Ar}), 8.41 (1H, s, H_{Ar}), 8.63 (2H, s, H_{Ar}), and 10.51 (15, s, NH). ^{13}C-NMR (75 MHz, DMSO-d_6) δ (ppm): 17.88, 18.68, 39.15, 39.43, 39.71, 39.98, 40.26, 40.54, 40.82, 128.13, 129.80, 131.99, 135.47, 143.78, 152.35, 179.31, and 181.66. Mass (ESI), *m/z*: 386.0813 (M^+). Anal. calcd. for C, 59.29; H, 4.45; Cl, 9.21; N, 14.56; O, 4.16; S, 8.33. Found: C, 59.30; H, 4.47; Cl, 9.22; N, 14.53; O, 4.18; S, 8.34.

*2-(1-(2-(4-Methoxyphenyl)-4-methylthiazole-5-yl)ethylidene)-N-methylhydrazinecarboxamide (**10**)*

Yield, 66–70%; m.p. 204.5°C. IR V_{max} (cm^{-1}): 3,361.7 (NH), 3,184.5–3,073 (arom.), 2,994.2–2,836.6 (aliph.), 1,677.31 (C═O), 1,536.16–1,518.39 (C═N, C═C), and 750.87 (C–S). ^{1}H-NMR (300 MHz, DMSO-d_6) δ (ppm): 2.27 (3H, s, CH_3), 2.62 (3H, s, CH_3), 3.83 (3H, s, OCH_3), 7.00–7.09 (3H, m, H_{Ar}), 7.27–7.33 (2H, m, H_{Ar}), 7.57–7.60 (2H, m, H_{Ar}), 7.86–7.91 (2H, m, H_{Ar}), 8.61 (1H, s, NH), and 9.97 (1H, s, NH). ^{13}C-NMR (75 MHz, DMSO-d_6) δ (ppm): 17.60, 18.54, 39.16, 39.44, 39.71, 39.99, 40.27, 40.55, 40.83, 55.89, 115.06, 119.14, 119.53, 122.96, 126.08, 128.07, 129.18, 139.32, 141.69, 151.06, 153.46, 161.47, and 164.24. Mass (ESI), *m/z*: 381.1378 (M^+). Anal. calcd. for C, 63.14; H, 5.30; N, 14.73; O, 8.41; S, 8.43. Found: C, 63.15; H, 5.33; N, 14.71; O, 8.40; S, 8.45.

*2-(1-(4-Methyl-2-(pyridine-2-yl)thiazole-5-yl)ethylidene)-N-phenylhydrazinecarboxamide (**11**)*

Yield, 68–70%; m.p. 250.1°C. IR V_{max} (cm^{-1}): 3,358.4 (NH), 3,184.5–3,086 (arom.), 2,928.5 (aliph.), 1,678.99 (C=O), 1,533.06 (C=N, C=C), and 742.22 (C–S). ^{1}H-NMR (300 MHz, DMSO-d_6) δ (ppm): 2.35 (H, s, CH_3), 2.68 (3H, s, CH_3), 7.03 (1H, t, J = 7.5 Hz, H_{Ar}), 7.31 (2H, t, J = 6 Hz, H_{Ar}), 7.47–7.51 (1H, m, H_{Ar}), 7.59 (2H, d, J = 9 Hz, H_{Ar}), 7.96 (1H, td, J = 9 Hz, H_{Ar}), 8.12 (1H, d, J = 9 Hz, H_{Ar}), 8.62 (1H, d, J = 9 Hz, H_{Ar}), 8.66 (1H, s, H_{Ar}), and 10.02 (1H, s, NH). ^{13}C-NMR (75 MHz, DMSO-d_6) δ (ppm): 17.86, 18.73, 39.16, 39.44, 39.72, 40.00, 40.27, 40.55, 40.83, 119.40, 119.61, 122.99, 125.60, 129.17, 134.39, 138.16, 139.32, 141.45, 150.22, 150.80, 151.71, 153.49, and 165.24. Mass (ESI), m/z: 352.1212 (M^+). Anal. calcd. for C, 61.52; H, 4.88; N, 19.93; O, 4.55; S, 9.12. Found: C, 61.54; H, 4.90; N, 19.91; O, 4.57; S, 9.15.

*2-(1-(4-Methyl-2-(pyridine-3-yl)thiazole-5-yl)ethylidene)-N-phenylhydrazinecarboxamide (**12**)*

Yield, 70–72%; m.p. 225.4°C. IR V_{max} (cm^{-1}): 3,368.3 (NH), 3,191–3,053.2 (arom.), 2,984.3–2,882.6 (aliph.), 1,692.73 (C=O), 1,523.86–1,499.71 (C=N, C=C), and 752.77 (C–S). ^{1}H-NMR (300 MHz, DMSO-d_6) δ (ppm): 2.35 (3H, s, CH_3), 2.67 (3H, s, CH_3), 7.03 (1H, t, J = 7.5Hz, H_{Ar}), 7.31 (2H, t, J = 6 Hz, H_{Ar}), 7.52–7.60 (3H, m, H_{Ar}), 8.30 (1H, dt, J = 9 Hz, H_{Ar}), 8.63 (1H, s, H_{Ar}), 8.68 (1H, dd, J = 6 Hz, H_{Ar}), 9.12 (1H, s, NH), and 10.04 (1H, s, NH). ^{13}C-NMR (75 MHz, DMSO-d_6) δ (ppm): 17.53, 18.46, 119.58, 123.01, 124.73, 129.18, 133.38, 133.81, 139.29, 141.28, 147.20, 151.41, 151.51, 153.38, and 161.17. Mass (ESI), m/z: 352.1219 (M^+). Anal. calcd. for C, 61.52; H, 4.88; N, 19.93; O, 4.55; S, 9.12. Found: C, 61.54; H, 4.90; N, 19.91; O, 4.57; S, 9.15.

*2-(1-(4-Methyl-2-(pyridine-4-yl)thiazole-5-yl)ethylidene)-N-phenylhydrazinecarboxamide (**13**)*

Yield, 66–70%; m.p. 240.6°C. IR V_{max} (cm^{-1}): 3,378.1 (NH), 3,194.3–3,079.5 (arom.), 2,984.3–2,885.9 (aliph.), 1,703.32 (C=O), 1,599.46–1,526.91 (C=N, C=C), 754.50 (C–S). ^{1}H-NMR (300 MHz, DMSO-d_6) δ (ppm): 2.36 (3H, s, CH_3), 2.68 (3H, s, CH_3), 7.03 (1H, t, J = 7.5 Hz, H_{Ar}), 7.31 (2 H, t, J = 6 Hz, H_{Ar}), 7.59 (2H, d, J = 9 Hz, H_{Ar}), 7.87 (2H, dd, J = 6 Hz, H_{Ar}), 8.65 (1H, s, H_{Ar}), 8.71 (2H, dd, J = 6 Hz, H_{Ar}), and 10.07 (1H, s, NH). ^{13}C-NMR (75 MHz, DMSO-d_6) δ (ppm): 17.54, 18.51, 119.27, 119.60, 120.21, 123.03, 129.18, 134.58, 139.28, 139.64, 139.70, 141.06, 151.22, 151.36, 151.89, 153.35, and 161.33. Mass (ESI), m/z: 352.1216 (M^+). Anal. calcd. for C, 61.52; H, 4.88; N, 19.93; O, 4.55; S, 9.12. Found: C, 61.54; H, 4.90; N, 19.91; O, 4.57; S, 9.15.

*2-(1-(4-Methyl-2-(pyrazine-2-yl)thiazole-5-yl)ethylidene)-N-phenylhydrazinecarboxamide (**14**)*

Yield, 72–74%; m.p. 210°C. IR V_{max} (cm^{-1}): 3,381.4 (NH), 3,197.6–3,092.6 (arom.), 2,984.3–2,902.3 (aliph.), 1,680.57 (C=O), 1,539.55–1,520.38 (C=N, C=C), and 760.19 (C–S). ^{1}H NMR (300 MHz, DMSO-d_6) δ (ppm): 2.36 (3H, s, CH_3), 2.70 (3H, s, CH_3), 7.03 (1H, t, J = 6 Hz, H_{Ar}), 7.31 (2H, t, J = 6 Hz, H_{Ar}), 7.58 (1H, d, J = 9 Hz, H_{Ar}), 8.67–8.75 (3H, m, H_{Ar}), 9.29 (1H, s, H_{Ar}), and 10.05 (1H, s, NH). ^{13}C NMR (75 MHz, DMSO-d_6) δ (ppm): 17.78, 18.67, 18.94, 119.65, 123.02, 125.12, 125.68, 128.71, 129.17, 139.30, 140.77, 141.14, 145.05, 146.21, 146.37, 152.18, 153.42, and 162.52. Mass (ESI), m/z: 353.1164 (M^+). Anal. calcd. for C, 57.94; H, 4.58; N, 23.85; O, 4.54, S, 9.10. Found: C, 57.96; H, 4.60; N, 23.83; O, 4.52, S, 9.09.

*2-(1-(4-Methyl-2-(pyrimidine-2-yl)thiazole-5-yl)ethylidene)-N-phenylhydrazinecarboxamide (**15**)*

Yield, 72–76%; m.p. 258.7°C. IR V_{max} (cm^{-1}): 3,358.4 (NH), 3,187.8–3,059.8 (arom.), 2,990.9–2,902.3 (aliph.), 1,678.90 (C=O), 1,554.89–1,531.72 (C=N, C=C), and 754.65 (C–S). ^{1}H NMR (300 MHz, DMSO-d_6) δ (ppm): 2.36 (3H, s, CH_3), 2.70 (3H, s, CH_3), 7.02 (1H, t, J = 6 Hz, H_{Ar}), 7.31 (2H, t, J = 6 Hz, H_{Ar}), 7.55–7.59 (3H, m, H_{Ar}), 8.69 (1H, m, H_{Ar}), 8.93 (2H, d, J = 3 Hz, H_{Ar}), 10.05 (1H, s, NH). ^{13}C NMR (75 MHz, DMSO-d_6) δ (ppm): 17.88, 18.79, 119.63, 121.97, 123.01, 129.17, 139.31, 141.15, 153.45, and 158.58. Mass (ESI), m/z: 353.1165 (M^+). Anal. calcd. for C, 57.94; H, 4.58; N, 23.85; O, 4.54, S, 9.10. Found: C, 57.96; H, 4.60; N, 23.83; O, 4.52, S, 9.09.

*2-(1-(4-Methyl-2-phenylthiazole-5-yl)ethylidene)-N-phenylhydrazinecarboxamide (**16**)*

Yield, 66–68%; m.p. 190.4°C. IR V_{max} (cm^{-1}): 33.61.7 (NH), 3,273.1–3,194.3 (arom.), 2,987.48–2,902.3 (aliph.), 1,684.8 (C=O), 1,637.40–1,489.28 (C=N, C=C), and 757.91 (C–S). ^{1}H-NMR (300 MHz, DMSO-d_6) δ (ppm): 2.34 (3H, s, CH_3), 2.65 (3H, s, CH_3), 7.02 (1H, t, J = 6 Hz, H_{Ar}), 7.30 (2H, t, J = 6 Hz, H_{Ar}), 7.51 (3H, m, H_{Ar}), 7.60 (2H, s, H_{Ar}), 7.91–7.99 (2H, m, H_{Ar}), 8.63 (1H, s, H_{Ar}), and 10.00 (1H, s, NH). ^{13}C NMR (75 MHz, DMSO-d_6) δ (ppm): 17.61, 18.55, 19.20, 119.56, 122.98, 126.43, 126.48, 126.65, 129.18, 129.72, 130.84, 131.10, 132.40, 133.10, 133.25, 139.31, 141.50, 153.44, and 166.19. Mass (ESI), m/z: 351.1258 (M^+). Anal. calcd. for C, 65.12; H, 5.18; N, 15.99; O, 4.57; S, 9.15. Found: C, 65.14; H, 5.20; N, 16.00; O 4.55; S, 9.12.

*2-(1-(2-(4-Chlorophenyl)-4-methylthiazole-5-yl)ethylidene)-N-methylhydrazinecarbothioamide (**17**)*

Yield, 72–76%; m.p. 117.9°C. IR V_{max} (cm^{-1}): 3,299.4 (NH), 3,092.6 (arom.), 2,990.9–2,925.3 (aliph.), 1,661.44 (C=N, C=C), 1,087.16 (C=S), and 649.80 (C–S). ^{1}H-NMR (300 MHz, DMSO-d_6) δ (ppm): 2.38 (3H, s, CH_3), 2.60 (3H, s, CH_3), 3.04 (3H, s, CH_3), 7.58 (2H, d, J = 8 Hz, H_{Ar}), 7.93 (2H, d, J = 8 Hz, H_{Ar}), 8.11 (1H, s, H_{Ar}), and 10.52 (1H, s, NH). ^{13}C NMR (75 MHz, DMSO-d_6) δ (ppm): 17.86, 18.56, 30.64, 31.65, 128.08, 128.74, 129.82, 131.98, 132.84, 135.44, 143.56, 152.25, 163.36, and 178.95. Mass (ESI), m/z: 340.0425 (M^+). Anal. calcd. for C, 49.62; H, 4.46; Cl, 10.46; N, 16.53; S, 18.92. Found: C, 49.64; H, 4.47; Cl, 10.43; N, 16.56; S, 18.94.

*2-(1-(2-(4-Methoxyphenyl)-4-methylthiazole-5-yl)ethylidene)-N-methylhydrazinecarbothioamide (**18**)*

Yield, 66–70%; m.p. 214.3°C. IR V_{max} (cm^{-1}): 3,371.6 (NH), 3,217.3–3,004 (arom.), 2,928.5–2,836.6 (aliph.), 1,609.3 (C=N, C=C), 1,054.37 (C=S), and 827.03 (C–S). ^{1}H-NMR (300 MHz,

DMSO-d_6) δ (ppm): 2.36 (3H, s, CH_3), 2.71 (3H, s, thiazole CH_3), 3.04 (3H, s, NCH_3), 3.82 (3H, s, OCH_3), 7.04 (2H, d, J = 8.53 Hz, phenyl $C_{3,5}$–H), and 7.84–7.87 (2H, d, J = 7.68 Hz, phenyl $C_{2,6}$–H). ^{13}C NMR (75 MHz, DMSO-d_6) δ (ppm): 17.88, 18.61, 31.61, 55.89, 115.06, 126.01, 128.07, 131.15, 143.94, 151.95, 161.53, 164.82, and 178.98. Mass (ESI), m/z: 335.0994 (M^+). Anal. calcd. for C, 53.87; H, 5.42; N, 16.75; O, 4.78; S, 19.17. Found: C, 53.88; H, 5.44; N, 16.72; O, 4.80; S, 19.19.

*N-Methyl-2-(1-(4-methyl-2-(pyridine-2-yl)thiazole-5-yl)ethylidene)-hydrazinecarbothioamide (**19**)*

Yield, 74–76%; m.p. 232.7°C. IR V_{max} (cm^{-1}): 3,358.4 (NH), 3,151.7 (arom.), 2,977.8–2,931.8 (aliph.), 1,544.81–1,502.98 (C═N, C═C), 1,049.43 (C═S), 782.89 (C–S). ^{1}H NMR (300 MHz, DMSO-d_6) δ (ppm): 2.39 (3H, s, CH_3), 2.62 (3H, s, thiazole CH_3), 3.04 (3H, s, NCH_3), 7.47–7.51 (1H, m, pyridine C_4–H), 7.95 (1H, t, J = 7.95 Hz, pyridine C_5–H), 8.11 (1H, d, J = 8.40 Hz, pyridine C_3–H), 8.13 (1H, brs, NH), and 8.61 (1H, d, pyridine C_6–H). ^{13}C NMR (75 MHz, DMSO-d_6) δ (ppm): 17.99, 18.74, 31.65, 19.46, 75.68, 134.40, 138.18, 143.69, 150.18, 150.73, 152.46, 165.94, and 179.04. Mass (ESI), m/z: 306.0837 (M^+). Anal. calcd. for C, 51.12; H, 4.95; N, 22.93; S, 21.00. Found: C, 51.10; H, 4.96; N, 22.10; S, 21.01.

*N-Methyl-2-(1-(4-methyl-2-(pyridine-3-yl)thiazole-5-yl)ethylidene)-hydrazinecarbothioamide (**20**)*

Yield, 66–70%; m.p. 209.8°C. IR V_{max} (cm^{-1}): 3,371.6 (NH), 3,148.4 (arom.), 2,971.2–2,905.6 (aliph.), 1,583–1,500.27 (C═N, C═C), 1,053.67 (C═S), and 705.01 (C–S). ^{1}H NMR (300 MHz, DMSO-d_6) δ (ppm): 2.39 (3H, s, CH_3), 2.62 (3H, s, thiazole CH_3), 3.04 (3H, s, NCH_3), 7.52–7.56 (1H, m, pyridine C_5–H), 8.09 (1H, s, NH), 8.26 (1H, d, J = 8.64 Hz, pyridine C_4–H), 8.66 (1H, d, J = 4.94 Hz, pyridine C_6–H), and 9.09 (1H, s, pyridine C_2–H). ^{13}C NMR (75 MHz, DMSO-d_6) δ (ppm): 17.90, 18.50, 31.64, 124.76, 129.16, 133.25, 133.80, 143.42, 147.17, 151.50, 152.35, 161.72, and 179.06. Mass (ESI), m/z: 306.0837 (M^+). Anal. calcd. for C, 51.12; H, 4.95; N, 22.93; S, 21.00. Found: C, 51.10; H, 4.96; N, 22.90; S, 21.01.

*N-Methyl-2-(1-(4-methyl-2-(pyridine-4-yl)thiazole-5-yl)ethylidene)-hydrazinecarbothioamide (**21**)*

Yield, 72–74%; m.p. 257.2°C. IR V_{max} (cm^{-1}): 3,368.3 (NH), 3,145.1–3,059.8 (arom.), 2,941.7–2,902.3 (aliph.), 1,599.5–1,515.61 (C═N, C═C), 1,057.63 (C═S), and 702.44 (C–S). ^{1}H NMR (300 MHz, DMSO-d_6) δ (ppm): 2.40 (3H, s, CH_3), 2.63 (3H, s, thiazole CH_3), 3.05 (3H, s, NCH_3), 7.84 (2H, d, J = 4.52 Hz, pyridine $C_{3,5}$–H), 8.13 (1H, brs, NH), 8.69 (2H, d, J = 4.52 Hz, pyridine $C_{2,6}$–H), and 10.53 (1H, s, NH). ^{13}C NMR (75 MHz, DMSO-d_6) δ (ppm): 17.90, 18.53, 31.66, 120.19, 134.45, 139.65, 143.17, 151.26, 152.69, 161.89, and 179.09. Mass (ESI), m/z: 306.0837 (M^+). Anal. calcd. for C, 51.12; H, 4.95; N, 22.93; S, 21.00. Found: C, 51.10; H, 4.96; N, 22.90; S, 21.01.

*N-Methyl-2-(1-(4-methyl-2-(pyrazine-2-yl)thiazole-5-yl)ethylidene)-hydrazinecarbothioamide (**22**)*

Yield, 74–78%; m.p. 210°C. IR V_{max} (cm^{-1}): 3,361.7 (NH), 3,227.2–3,043.4 (arom.), 2,987.6–2,931.8 (aliph.), 1,680.57 (C═O), 1,655.2–1,496.61 (C═N, C═C), 1,049.08 (C═S), and 755.03 (C–S). ^{1}H NMR (300 MHz, DMSO-d_6) δ (ppm): 2.40 (3H, s, CH_3), 2.64 (3H, s, thiazole CH_3), 3.03 (3H, s, NCH_3), 8.15 (1H, brs, NH), 8.69–8.71 (1H, m, piperazine C_5–H), 8.91 (1H, d, J = 2.45 Hz, piperazine C_6–H), 8.92 (1H, d, J = 1.60 Hz, pyrazine C_3–H), and 10.49 (1H, s, NH). ^{13}C NMR (75 MHz, DMSO-d_6) δ (ppm): 17.93, 18.67, 31.68, 135.49, 140.80, 143.30, 145.01, 146.13, 146.29, 152.90, 163.2, and 179.06. Mass (ESI), m/z: 307.0791 (M^+). Anal. calcd. for C, 47.04; H, 4.61; N, 27.43; S, 20.93. Found: C, 47.01; H, 4.62; N, 27.45; O, 4.52, S, 20.94.

*N-Methyl-2-(1-(4-methyl-2-(pyridine-2-yl)thiazole-5-yl)ethylidene)-hydrazinecarbothioamide (**23**)*

Yield, 68–70%; m.p. 216.3°C. IR V_{max} (cm^{-1}): 3,365 (NH), 3,155 (arom.), 2,997.4–2,908.8 (aliph.), 1,523.30–1,496.72 (C═N, C═C), 1,124.02 (C═S), and 797.92 (C–S). ^{1}H NMR (300 MHz, DMSO-d_6) δ (ppm): 2.40 (3H, s, CH_3), 2.64 (3H, s, thiazole CH_3), 3.04 (3H, s, NCH_3), 8.15 (1H, brs, NH), 8.69–8.71 (1H, m, pyrimidine C_5–H), 8.92 (2H, d, J = 4.85 Hz, pyrimidine $C_{4,6}$–H), 10.49 (1H, s, NH). ^{13}C NMR (125 MHz, DMSO-d_6) δ (ppm): 18.03, 18.76, 31.68, 122.03, 136.01, 143.33, 153.14, 158.56, 158.93, 163.38, and 179.07. Mass (ESI), m/z: 307.0795 (M^+). Anal. calcd. for C, 47.04; H, 4.61; N, 27.43; S, 20.93. Found: C, 47.01; H, 4.60; N, 27.44; S, 20.91.

*N-Methyl-2-(1-(4-methyl-2-phenylthiazole-5-yl)ethylidene)hydrazinecarbothioamide (**24**)*

Yield, 64–66%; m.p. 219.4°C. IR V_{max} (cm^{-1}): 3,358.4 (NH), 3,171.4 (arom.), 2,974.5–2,902.3 (aliph.), 1,520.04–1,491.79 (C═N, C═C), 1,052.52 (C═S), and 761.54 (C–S). ^{1}H NMR (300 MHz, DMSO-d_6) δ (ppm): 2.38 (3H, s, CH_3), 2.60 (3H, s, thiazole CH_3), 3.03 (3H, s, NCH_3), 7.48–7.52 (3H, m, phenyl $C_{3,4,5}$–H), 7.91–7.94 (2H, m, phenyl $C_{2,6}$–H), 8.07 (1H, brs, NH), and 10.46 (1H, s, NH). ^{13}C NMR (75 MHz, DMSO-d_6) δ (ppm): 17.93, 18.59, 31.63, 126.42, 129.73, 130.93, 132.29, 133.19, 143.71, 152.15, 164.79, and 179.03. Mass (ESI), m/z: 305.0879 (M^+). Anal. calcd. for C, 55.23; H, 5.30; N, 18.40; S, 21.07. Found: C, 55.21; H, 5.32; N, 18.39; S, 21.04.

4.2 | Anticancer activity

The effect of the compounds on cellular proliferation was monitored using the cell proliferation reagent kit I (MTT, 3-(4,5-dimethylthiazol-2-yl)-2,5-diphenyltetrazolium bromide; Roche Applied Science, Catalog Number: 11465007001).[48,49] The HEK293 (American Type Culture Collection, Manassas, VA) and MCF7 (American Type Culture Collection) cell lines were seeded in 100 µl of growth medium at a density of 5×10^3 cells/well in 96-well plates and allowed to adhere for 24 hr. Then, serially diluted compounds were added to an additional 100 µl of growth medium. The cells were incubated for 48 hr at 37°C in humidified 5% CO_2. After incubation, 10 µl of MTT stock solution was added to each well and further

incubated at 37°C for 4 hr. Then, 100 μl of solubilizing solution was added, and the plates were read at 550–600 nm using a scanning multiwell spectrophotometer. The results were expressed as a percentage of the control based on the means of three replicates. The IC_{50} cytotoxicity values were determined as the compound concentration that reduced the absorbance to 50% of that in the untreated control wells.

4.3 | Ribonucleotide reductase enzyme assay

Ribonucleotide reductase enzyme inhibition was monitored using the RRM2 ELISA Kit (MyBioSource, ABD). The synthesized compounds were first dissolved (under 1%) in dimethyl sulfoxide. Under sterile conditions, the HEK293 cell lines were cultured and collected separately for each compound in the amount appropriate for the kit content, and then transferred from the wells to microcentrifuge tubes. The cell suspension was diluted with 1× PBS (pH 7.2–7.4) until the cell concentration reached 100 million/ml. The cells were stored overnight at −20°C. After two freeze-thaw cycles to break up the cell membranes, the cell lysates were centrifuged for 5 min at 5,000*g*, 2–8°C. The supernatant was collected, and the enzyme activity of all compounds was evaluated in accordance with the manufacturer's instructions.

4.4 | Theoretical calculation of the ADME parameters

The physicochemical parameters of molecular weight, tPSA, number of hydrogen donors, number of hydrogen acceptors, number of rotatable bonds and volume were analyzed for all compounds using the online Molinspiration property calculator.[46] Drug-likeness properties of the compounds were calculated using the QikProp module of Maestro (Schrodinger Inc.).

4.5 | Spectrophotometric determination of complex formation

Absorption measurements were carried out using an Agilent 8453 model UV-Vis spectrophotometer with a 1.00-cm quartz cell. The experiments were performed at a wavelength of 190 to 800 nm. An Oakton pH 2100 series pH-meter was used in combination with a glass electrode for pH measurements. All the ligands were used without further purification. All chemicals and buffer used were of reagent or spectral grade purity. $NaH_2PO_4{\cdot}2H_2O$ and Na_2HPO_4 were supplied by Sigma-Aldrich, and ethanol and acetonitrile were purchased from Merck. Ferric nitrate nonahydrate was supplied by Riedel-de Haen. 0.1 mM standard solutions of various ligands and ferric nitrate were dissolved in ethanol and metisazone was dissolved in acetonitrile. All these solutions were used as stock solutions throughout the study. The acidity of the solution was kept constant at pH 7.40 within a buffer solution containing NaH_2PO_4/Na_2HPO_4 having 0.1 M ionic strength. The stoichiometric ratio of the ligand–metal complex was determined using the mole ratio technique.[50] Blanks were prepared by mixing 1 ml of ethanol and 9 ml of buffer. In the mole ratio method, ligand–metal solutions were buffered at pH 7.4. The ratio (moles of ligand/moles of metal) ranged from 0.5 to 5.0, in which the amount of metal was kept constant but that of the ligand varied. The absorbance values of the complex were measured immediately after mixing the ligand and metal at room temperature. For each solution, absorbance at λ_{max} was plotted against the mole ratio (n_L/n_M).

4.6 | Molecular modeling studies

4.6.1 | Ligand preparation and docking experiment

The preparation of the protein structure and ligand, binding site mapping, GRID files, docking, and scoring were performed using algorithms included in the Maestro modules (Schrodinger Inc.). The X-ray crystallographic structure of human ribonucleotide reductase (PDB entry code: 1W68) was obtained from the Protein Data Bank (RCSB).[51] The 1W68 PDB file was edited using the protein preparation wizard from the Workflows menu (Maestro) for hydrogen insertion and rotamer adjustment, and H-bond optimization using OPLS 3e as the energy parameters. The 3D diagrams of the synthesized compounds were drawn and inspected using the 3D builder implemented in the Maestro suite (Schrödinger LCC, OR). These compounds were prepared and minimized by means of the OPLS 3e force field and the partial atomic charges, ionization and tautomerization states were computed at a pH range of 6–8 by Epik using the LigPrep module of the same suite. Then they were subjected to a docking experiments to identify the probable interactions between the ligands and the enzyme-active site by using the Glide module in Schrodinger. The standard precision protocol included in Glide was employed with the default parameter settings to the most probable site near iron atoms found by the site map function of the same software. The highest e-model scoring poses of the compounds were selected for further evaluation to explain the probable ligand–enzyme interactions.

ACKNOWLEDGMENT

This study was supported by the Anadolu University Scientific Research Projects Commission, Eskisehir, Turkey (project number: 1609S624).

CONFLICT OF INTERESTS

The authors declare that there are no conflict of interests.

ORCID

Merve Ertas http://orcid.org/0000-0002-2289-7950
Barkin Berk http://orcid.org/0000-0001-6047-2796
Leyla Yurttas http://orcid.org/0000-0002-0957-6044

REFERENCES

[1] P. V. Bernhardt, P. C. Sharpe, M. Islam, D. B. Lovejoy, D. S. Kalinowski, D. R. Richardson, *J. Med. Chem.* **2009**, *52*, 407.
[2] N. C. Andrews, *N. Engl. J. Med.* **1999**, *341*, 1986.
[3] T. C. Iancu, H. Shiloh, A. Kedar, *Cancer* **1988**, *61*, 2497.
[4] K. P. Hoyes, R. C. Hider, J. B. Porter, *Cancer Res.* **1992**, *52*, 4591.
[5] N. T. Le, D. R. Richardson, *Biochim. Biophys. Acta.* **2002**, *1603*, 31.
[6] A. C. Sartorelli, K. C. Agrawal, A. S. Tsiftsoglou, A. E. Moore, *Adv. Enzyme Regul.* **1977**, *15*, 117.
[7] H. L. Elford, M. Freese, E. Passamani, H. P. Morris, *J. Med. Chem.* **1970**, *245*, 5228.
[8] J. G. Cory, P. Chiba, in *Inhibitor of Ribonucleotide Diphosphate Reductase Activity*, Pergamon Press, Oxford, UK **1989**, pp. 245–264.
[9] G. Pelosi, *J. Open Crystallogr.* **2010**, *3*, 16.
[10] I. Đilović, M. Rubčić, V. Vrdoljak, S. K. Pavelić, M. Kralj, I. Piantanida, M. Cindrić, *Bioorg. Med. Chem.* **2008**, *16*, 5189.
[11] Z. Kovacevic, S. Chikhani, G. Y. L. Lui, S. Sivagurunathan, D. R. Richardson, *Antioxid. Redox. Signal.* **2013**, *18*, 874.
[12] G. Domagk, R. Behnisch, F. Mietzsch, H. S. Schmidt, *Naturwissenschaften* **1946**, *33*, 315.
[13] A. S. Dobek, D. L. Klayman, E. T. Dickson, J. P. Scovill, C. N. Oster, *Drug Res.* **1983**, *33*, 1583.
[14] D. L. Klayman, J. P. Scovill, J. F. Bartosevich, C. J. Mason, *J. Med. Chem.* **1979**, *22*, 1367.
[15] D. L. Klayman, J. P. Scovill, C. J. Mason, J. F. Bartosevich, J. Bruce, A. Lin, *Drug Res.* **1983**, *33*, 909.
[16] C. Shipman, S. H. Smith, J. C. Drach, D. L. Klayman, *Antiviral Res.* **1986**, *6*, 197.
[17] F. A. French, E. J. Blanz, J. R. DoAmaral, D. A. French, *J. Med. Chem.* **1970**, *13*, 1117.
[18] J. F. de Oliveira, T. S. Lima, D. B. Vendramini-Costa, S. C. B. de Lacerda Pedrosa, E. A. Lafayette, R. M. F. da Silva, S. M. V. de Almeida, R. O. de Moura, A. L. T. G. Ruiz, J. E. de Carvalho, M. C. A. de Lima, *Eur. J. Med. Chem.* **2017**, *136*, 305.
[19] Y. G. Goan, B. Zhou, E. Hu, S. Mi, Y. Yen, *Cancer Res.* **1999**, *59*, 4204.
[20] M. C. Liu, T. C. Lin, A. C. Sartorelli, *J. Med. Chem.* **1992**, *35*, 3672.
[21] J. Easmon, G. Pürstinger, G. Heinisch, T. Roth, H. H. Fiebig, W. Holzer, W. Jäger, M. Jenny, J. Hofmann, *J. Med. Chem.* **2001**, *44*, 2164.
[22] A. Y. Lukmantara, D. S. Kalinowski, N. Kumar, D. R. Richardson, *Bioorg. Med. Chem. Lett.* **2013**, *23*, 967.
[23] Y. Yu, Y. S. Rahmanto, D. Richardson, *Br. J. Pharmacol.* **2012**, *165*, 148.
[24] D. R. Richardson, P. C. Sharpe, D. B. Lovejoy, D. Senaratne, D. S. Kalinowski, M. Islam, P. V. Bernhardt, *J. Med. Chem.* **2006**, *49*, 6510.
[25] J. Yuan, D. B. Lovejoy, D. R. Richardson, *Blood* **2004**, *104*, 1450.
[26] M. Whitnall, J. Howard, P. Ponka, D. R. Richardson, *Proc. Natl. Acad. Sci.* **2006**, *103*, 14901.
[27] P. Yogeeswari, D. Sriram, L. R. J. Sunil Jit, S. S. Kumar, J. P. Stables, *Eur. J. Med. Chem.* **2002**, *37*, 231.
[28] T. Siatra-Papastaikoudi, A. Tsotinis, C. Raptopoulou, C. Sambani, H. Thomou, *Eur. J. Med. Chem.* **1995**, *30*, 107.
[29] S. Saeed, N. Rashid, P. G. Jones, M. Ali, R. Hussain, *Eur. J. Med. Chem.* **2010**, *45*, 1323.
[30] W. Hu, W. Zhou, C. Xia, X. Wen, *Bioorg. Med. Chem. Lett.* **2006**, *16*, 2213.
[31] F. A. French, E. J. Blanz Jr, S. C. Shaddix, R. W. Brockman, *J. Med. Chem.* **1974**, *17*, 172.
[32] M. B. Bhalerao, S. T. Dhumal, A. R. Deshmukh, L. U. Nawale, V. Khedkar, D. Sarkar, R. A. Mane, *Bioorg. Med. Chem.* **2017**, *27*, 288.
[33] (a) W. E. Levinson, *Antimicrob. Chem.* **1980**, *1980*, 288; (b) L. A. Saryan, K. Mailer, C. Krishnamurti, W. Antholine, D. H. Petering, *Biochem. Pharmacol.* **1981**, *30*, 1595.
[34] D. R. Richardson, P. V. Bernhardt, *J. Biol. Inorg. Chem.* **1999**, *4*, 266.
[35] C. M. Armstrong, P. V. Bernhardt, P. Chin, D. R. Richardson, *Eur. J. Inorg. Chem.* **2003**, *114*, 5.
[36] D. R. Richardson, P. C. Sharpe, D. B. Lovejoy, D. Senaratne, D. S. Kalinowski, M. Islam, P. V. Bernhardt, *J. Med. Chem.* **2006**, *49*, 6510.
[37] J. C. Logan, M. P. Fox, J. H. Morgan, A. M. Makohon, C. J. Pfau, *J. Gen. Virol.* **1975**, *28*, 271.
[38] P. Reichard, A. Ehrenberg, *Science* **1983**, *221*, 514.
[39] C. H. Baker, J. Banzon, J. M. Bollinger, J. Stubbe, V. Samano, M. J. Robins, B. Lippert, E. Jarvi, R. Resvick, *J. Med. Chem.* **1991**, *34*, 1879.
[40] E. S. Casper, M. R. Green, T. D. Brown, D. P. Kelsen, T. Kresek, B. Trochanowski, *Invest. New Drugs* **1994**, *12*, 29.
[41] J. R. McCarthy, P. S. Sunkara, in *Chemical and Structural Approaches to Rational Drug Design* (Eds: D. B. Weiner, W. V. Williams), CRC Press, Boca Raton, FL **1994**, pp. 3–34.
[42] J. A. Wright, A. K. Chan, B. K. Choy, R. A. R. Hurta, G. A. McClarty, A. Y. Tagger, *Biochem. Cell. Biol.* **1990**, *68*, 1364.
[43] J. G. Cory, A. H. Cory, G. Rappa, A. Lorico, L. Mao-Chin, L. Tai-Shun, A. C. Sartorelli, *Biochem. Pharmacol.* **1994**, *48*, 335.
[44] B. Shakya, P. N. Yadav, J. Ueda, S. Awale, *Bioorg. Med. Chem. Lett.* **2014**, *24*, 458.
[45] H. van de Waterbeemd, E. Gifford, *Nat. Rev. Drug Discov.* **2003**, *2*, 192.
[46] Molinspiration Cheminformatics. Bratislava, Slovak Republic. Retrieved from www.molinspiration.com/services/properties.html
[47] C. A. Lipinski, F. Lombardo, B. W. Dominy, P. J. Feeney, *Adv. Drug. Deliv. Rev.* **2001**, *46*, 3.
[48] X. Shi, M. Sun, H. Liu, Y. Yao, R. Kong, F. Chen, Y. Song, *Mol. Carcinog.* **2015**, *54*, E1. https://doi.org/10.1002/mc.22120
[49] J. H. Park, S. J. Kim, E. J. Oh, S. Y. Moon, S. I. Roh, C. G. Kim, H. S. Yoon, *Biol. Reprod.* **2003**, *69*, 2007. https://doi.org/10.1095/biolreprod.103.017467
[50] J. Kuljanin, I. Janković, J. Nedeljković, D. Prstojević, V. Marinković, *J. Pharm. Biomed. Anal.* **2002**, *28*, 1215.
[51] K. R. Strand, S. Karlsen, M. Kolberg, Å. K. Røhr, C. H. Görbitz, K. K. Andersson, *J. Biol. Chem.* **2004**, *279*, 46794.

SUPPORTING INFORMATION

Additional supporting information may be found online in the Supporting Information section.

How to cite this article: Ertas M, Sahin Z, Bulbul EF, et al. Potent ribonucleotide reductase inhibitors: Thiazole-containing thiosemicarbazone derivatives. *Arch Pharm Chem Life Sci*. 2019;352:1900033. https://doi.org/10.1002/ardp.201900033